



PAPER

[View Article Online](#)
[View Journal](#) | [View Issue](#)Cite this: *Dalton Trans.*, 2021, **50**,
6204

Synthesis of pyrazole anchored three-coordinated organoboranes and their application in the detection of picric acid†

Shreenibasa Sa,^{‡a} Vanga Mukundam,^{‡a} Anupa Kumari,^b Ritwick Das ^{*b} and
Krishnan Venkatasubbaiah ^{*a}

Three-coordinated organoboron fluorophores bearing 3,5-diphenyl pyrazoles have been synthesized. The pyrazole anchored boron fluorophores show selective fluorescence quenching response to trinitrophenol (or) picric acid (PA) and have the ability to discriminate picric acid over other analytes. We investigated nonlinear optical (NLO) properties of these three-coordinated organoboron compounds (in solutions) in the presence and absence of PA. In absence of PA, the two-photon-absorption coefficient (β) of organoboron fluorophores exhibits a variation from $2 \times 10^{-12} \text{ cm W}^{-1}$ to $4 \times 10^{-12} \text{ cm W}^{-1}$. The results also reveal that the NLO characteristics of organoboron fluorophores exhibit a discernible variation with PA addition which has correlations with quenching observed in fluorescence measurements.

Received 22nd February 2021,
Accepted 9th April 2021

DOI: 10.1039/d1dt00586c

rsc.li/dalton

Introduction

Three-coordinated organoboranes are an important class of compounds which possess a vacant p-orbital through which they can establish interaction with an organic π -system and consequently could serve as a π -acceptor. Furthermore, the empty p-orbital of boron extends the π -conjugation in organic systems, which leads to unique absorption and emission properties. These unusual properties which are facilitated by interactions with boron compounds have been exploited in many opto-electronic applications.^{1–4} For instance, Marder, Lambert, Fang, Mullen, Jäkle and Perry have carried out extensive studies of such chromophores in the context of non-linear optics.^{5–9} Shirota and others have demonstrated the use of tri-coordinated boranes for realizing electron transport as well as efficient emitters.¹⁰ Wang, Yamaguchi, Tamao and others have shown that tri-coordinated boron compounds could be employed for realizing effective fluorescent and colorimetric sensors for the detection of fluoride anion.¹¹

The recognition and sensing of nitro-explosives has attracted substantial attention owing to ever-increasing

usage in terrorism related activities. Among the nitro explosives 2,4,6-trinitrophenol (picric acid, PA) shown superior explosive capabilities as compared to its counterpart trinitrotoluene (TNT).¹² Furthermore, picric acid can create severe health problems such as skin irritation, skin allergies, nausea and damage to respiratory organs.¹³ Hence, selective, reliable and convenient detection of picric acid is in high demand. Even though various fluorescent sensors, such as polymers, nanoparticles, mesoporous and metal organic frameworks have been reported for the detection of nitro-aromatic explosives, most of these investigations were directed towards the detection of TNT and discernibly weaker importance was given to the more powerful explosive picric acid.¹⁴ Although ample reports exist for the detection of picric acid, owing to similar electron affinities of poly nitro-aromatics, the augmentation of an effective and reliable sensor for picric acid with high selectivity is still a challenging task. We propose a very efficient and selective sensor based on tri-coordinated boron. To the best of our knowledge this is the first example of the use of tri-coordinated borane based fluorophores for the selective detection of picric acid.

Tri-coordinated boron has been chosen as the fluorophore unit because of its widely studied properties as discussed *vide supra*. A pyrazole unit at the *para* position of the phenyl ring or 5-position of thiophene was placed to act as an H-bond accepting site. We anticipate that the lone pair on the pyrazole nitrogen will help in forming H-bonding with picric acid through $\text{N} \cdots \text{H}-\text{O}$ interaction and consequently it would help to detect the picric acid selectively.

^aSchool of Chemical Sciences, National Institute of Science Education and Research (NISER), HBNI, Bhubaneswar-752050, Odisha, India. E-mail: krishnv@niser.ac.in^bSchool of Physical Sciences, National Institute of Science Education and Research (NISER), HBNI, Bhubaneswar-752050, Odisha, India

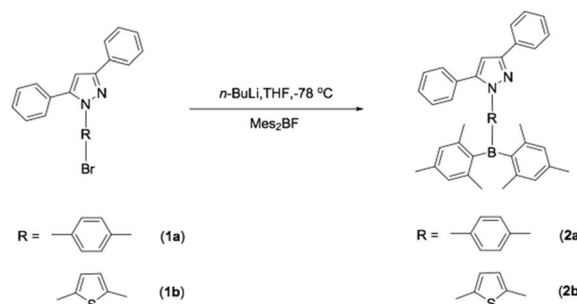
†Electronic supplementary information (ESI) available. CCDC 2063185 and 2063186. For ESI and crystallographic data in CIF or other electronic format see DOI: 10.1039/d1dt00586c

‡These authors contributed equally.

Results and discussion

Synthesis & characterisation

The starting material 1-(4-bromophenyl)-3,5-diphenyl-1*H*-pyrazole (**1a**) was prepared by following the literature reported procedure¹⁵ and compound **1b** was synthesized by Cu₂O catalyzed Ullmann-type coupling reaction of 3,5-diphenyl pyrazole and 2-bromothiophene followed by bromination using *N*-bromosuccinimide (ESI†). Compound **1a** or **1b** was reacted with *n*-butyllithium, then quenched with dimesitylboron fluoride, which yields the desired triaryl borane-pyrazole compounds **2a** and **2b** in 73 and 55% respectively (Scheme 1). The formation of compounds **2a** and **2b** were confirmed using ¹H, ¹³C and ¹¹B NMR spectroscopy. Compounds **2a** and **2b** were further characterized using single crystal X-ray diffraction crystallography (Fig. 1 & Table S2†). Compounds **2a** and **2b** crystallizes in the monoclinic *P*₂₁/*n* and *P*₂₁/*c* space groups respectively. The boron centre adopts a trigonal planar geometry (*S*_{C–B–C} = 359.9° for **2a** & 360.0° for **2b**) as shown in Fig. 1. The boron–carbon bond distances (1.572(2)–1.583(2) Å for **2a** and 1.538(3)–1.579(3) Å for **2b**) are comparable to the literature reported analogues tri-coordinated boron compounds.



Scheme 1 Synthetic route to the compounds **2a** & **2b**.

Photophysical properties

The absorption spectra of compound **2a** shows a weak solvatochromism, however the emission spectra exhibit strong solvatochromism (Fig. S1†). The emission maxima shifted from $\lambda_{em} = 370$ nm (toluene) to $\lambda_{em} = 403$ nm (CH₃CN), and the Stokes shift increases from 2913 cm⁻¹ to 5673 cm⁻¹ with increasing solvent polarity which indicates the presence of different charge distribution in the excited state in polar solvents compared to the ground state. The emission spectra of

Compound	X-ray	LUMO	HOMO
2a		 -1.822(eV)	 -5.794(eV)
2b		 -1.921(eV)	 -5.707(eV)

Fig. 1 (left) Molecular structures of **2a** and **2b**. Hydrogen atoms are omitted for clarity. (right) Computed orbitals for compounds **2a** and **2b**.

compound **2b** did not show any solvatochromism, however, its absorption spectra showed weak solvatochromism. The absorption and emission maxima of compound **2b** (358 nm & 415 nm in CH₃CN) exhibits a slight red shift (Fig. S1 & S2†) in comparison with compound **2a** (328 nm & 403 nm in CH₃CN) which is attributed due to electron donating nature of thiophene (Fig. 2). Cyclic voltammetry studies showed a reversible reduction wave for both **2a** and **2b** (Fig. S3†). Compound **2b** ($E_{1/2} = -2.42$ V) showed more negative potential than com-

pound **2a** ($E_{1/2} = -2.27$ V). The quantum yield for compounds **2a** & **2b** are 0.23 & 0.15 (in THF) respectively (Table S1†) which are comparable with other reported pyrazole based systems.^{14k} To better understand the photophysical properties of compounds **2a** and **2b**, theoretical calculations were performed.

As shown in Fig. 1, the HOMO of compounds **2a** and **2b** are dominated by the orbitals from the pyrazole, one of the phenyl ring with small dihedral angle attached to the pyrazole (the dihedral angles between the pyrazole and the phenyl rings are 46.0 & 5.0 for **2a**; 50.7 & 4.3° for **2b**) and the spacer ('phenyl' in case of **2a** and 'thiophene' in case of **2b**); whereas the LUMO gets in maximum contribution from the boron and the spacer (phenyl or thiophene) indicates that the pyrazole unit is the donor and the boron moiety acts as an acceptor. With this well-defined triarylborane anchored pyrazole in hand, we examined the application of compound **2a** as a probe for picric acid detection in THF. As shown in Fig. 3, gradual addition of picric acid to a solution of compound **2a** in THF causes substantial quenching of the emission. Addition of 14 equiv. (140 μ M) solution of picric acid quenches about 89% and 44% of emission intensity for the compounds **2a** and **2b** respectively (Fig. 3 and Fig. S4†). It is worth noting that 90% fluorescence quenching was observed for **2a** at 14 equiv. of PA and that for the **2b** it was observed at 70 equiv. of PA in THF. As picric acid is freely soluble in water, determination of PA in aqueous medium is necessary. Both the compounds **2a** and **2b** are not soluble in water; in order to use them in aqueous environment, mixed solvent system was adopted (THF:H₂O; 70:30) for further sensing studies. Aliquots of PA in water was added to compounds **2a** and **2b** in THF/H₂O (70:30) as described *vide supra*. About ~20% emission quenching was realized for **2a** & **2b**, upon addition of 0.5 equiv. of picric acid in H₂O. The emission further quenched to ~90% upon further addition of PA (92% quenching was observed for **2a** at 7 equiv. of PA and 90% quenching was observed for **2b** at 4.4 equiv. of PA) to compounds **2a** and **2b** respectively (see Fig. 4). We further studied the fluorescence quenching of compounds **2a** and **2b** using Stern–Volmer plot. At lower concentration of

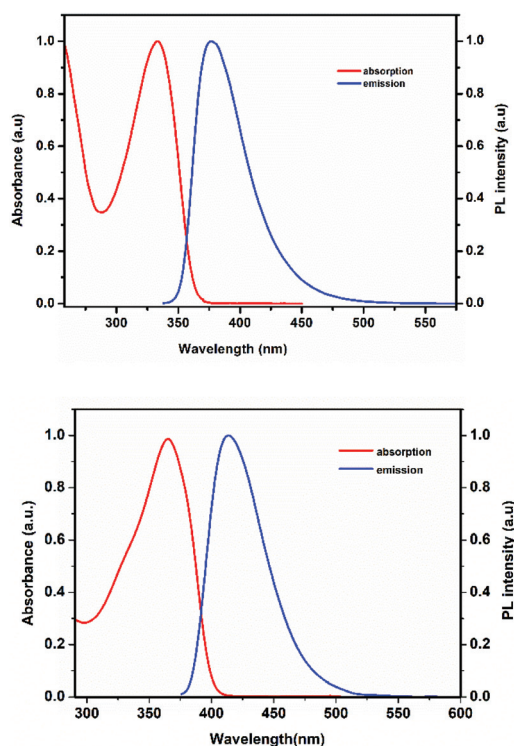


Fig. 2 Normalized UV-Vis absorption and fluorescence spectra of compounds **2a** (top) and **2b** (bottom). (Concentration = 10^{-5} M).

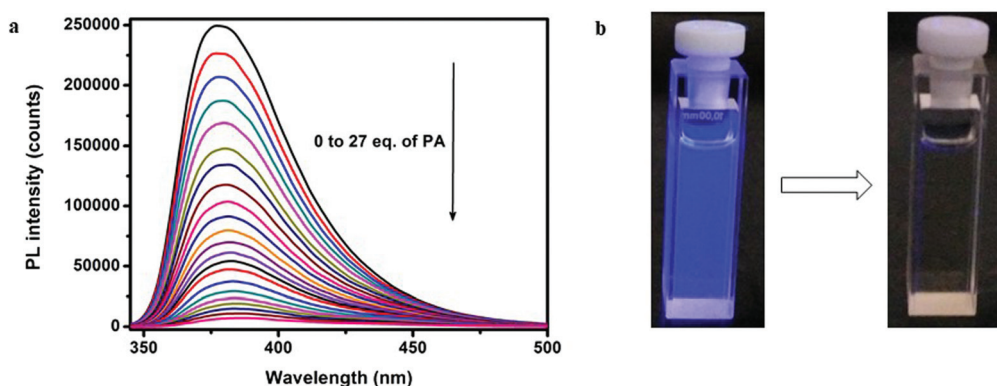


Fig. 3 (a) Fluorescence quenching of compound **2a** with the addition of different concentrations of PA (0, 0.25, 0.5, 0.75, 1.0, 1.5, 2.0, 3.0, 4.0, 5.0, 6.0, 7.0, 8.0, 9.0, 10.0, 12.0, 14.0, 16.0, 18.0, 23.0, and 27.0 equiv. of PA) in THF (10^{-5} M; excited at 333 nm). (b) Color change under a UV lamp before (left) and after (right) the addition of PA.

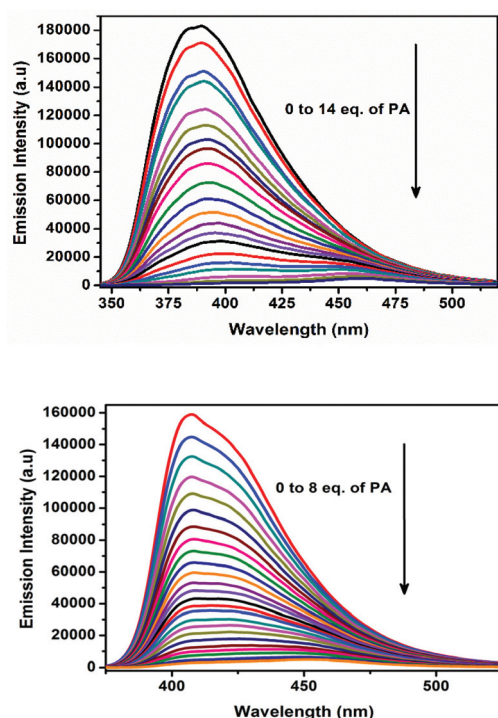


Fig. 4 (top) Fluorescence quenching of compound **2a** (10^{-5} M, excited at 333 nm) in a mixed solvent of THF : H₂O (70 : 30) with different concentrations of PA (0, 0.25, 0.5, 0.75, 1.0, 1.25, 1.50, 1.75, 2.0, 2.5, 3.0, 3.5, 4.0, 4.5, 5.0, 6.0, 7.0, 10.0, 12.0, and 14.0 equiv. of PA). (bottom) Fluorescence quenching of compound **2b** (10^{-5} M, excited at 366 nm) in a mixed solvent of THF : H₂O (70 : 30) with different concentrations of PA (0, 0.2, 0.4, 0.6, 0.8, 1.0, 1.2, 1.4, 1.6, 1.8, 2.0, 2.2, 2.4, 2.6, 2.8, 3.0, 3.3, 3.6, 4.0, 4.4, 5.0, 5.5, 6.0, 7.0 and 8.0 equiv. of PA).

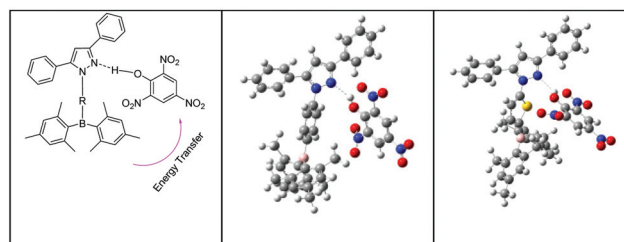
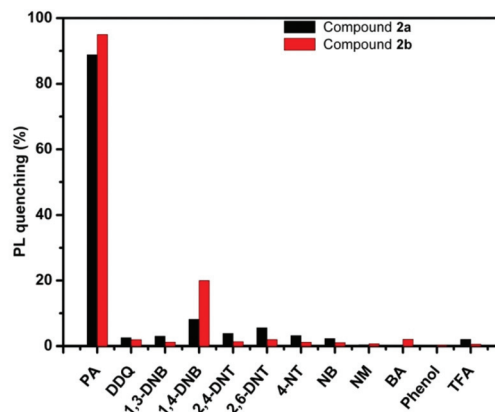


Fig. 5 (top) Fluorescence quenching efficiencies of compounds **2a** and **2b** in THF : H₂O (70 : 30) (10^{-5} M; excited at 333 nm) toward different nitroaromatics and other analytes (6 equiv.) like picric acid (PA), 1,3-dinitrobenzene (1,3-DNB), 1,4-dinitrobenzene (1,4-DNB), 2,4-dinitrotoluene (2,4-DNT), 2,6-dinitrotoluene (2,6-DNT), 4-nitrotoluene (4-NT), nitrobenzene (NB), DDQ, nitromethane (NM), benzoic acid (BA), phenol and trifluoroacetic acid (TFA). (bottom) Proposed quenching mechanism and optimized geometries of **2a-PA** & **2b-PA** (H-bond interaction for **2a** is H...N 1.982 Å; O—H...N 136.3° and for **2b** is H...N 2.177 Å; O—H...N 124.3°).

picric acid, the quenching constant was calculated using Stern–Volmer plot and was found to be $5.2 \times 10^4 \text{ M}^{-1}$ and $0.5 \times 10^4 \text{ M}^{-1}$ for compounds **2a** and **2b** in THF (Fig. S5 and S6†) respectively which confirms the high sensitivity of both the compounds towards picric acid in THF, whereas quenching constant is $5.4 \times 10^4 \text{ M}^{-1}$ for **2a** in THF : H₂O (70 : 30) and $6.1 \times 10^4 \text{ M}^{-1}$ for **2b** in THF : H₂O (70 : 30) (Fig. S7 and S8†). Time-resolved fluorescence measurements were carried out to realize the origin of the quenching process. As shown in the ESI,† the fluorescence life time of **2a** and **2b** is invariant in the presence of picric acid, which suggests that the mechanism of quenching is static (Fig. S9 and S10†). In order to judge the selectivity of compounds **2a** & **2b**, fluorescence response of the probes with different nitroaromatics (Fig. 5) and other analytes such as 1,3-dinitrobenzene (1,3-DNB), 1,4-dinitrobenzene (1,4-DNB), 2,4-dinitrotoluene (2,4-DNT), 2,6-dinitrotoluene (2,6-DNT), 4-nitrotoluene (4-NT), nitrobenzene (NB), DDQ, nitromethane (NM), benzoic acid (BA), phenol and trifluoroacetic acid (TFA) were studied. Among the different nitroaromatics and analytes tested, picric acid results in 90% quenching of emission of the probes (**2a** & **2b**), however the emission (**2a** & **2b**) quenching by other analytes was negligible. The selective emission response towards picric acid indicates that there is

an interaction between compound **2a** or **2b** and picric acid. In general, pyrazoles are prone to form hydrogen bonding with themselves through N—H...N intermolecular hydrogen bonding and with other molecules through intramolecular hydrogen bonding (N...H—X; X may be O or N). We propose that N...H—O interaction between compound **2a** or **2b** and picric acid resulted in selective fluorescence quenching (Fig. 5). Compounds **2a** & **2b** showed a much better or comparable detection limits compared to other fluorescent probes reported in the literature (Tables S3 & S4†).

To get deeper insight into the quenching mechanism, we carried out ¹H NMR studies of compound **2a** in DMSO-d₆. In the presence of picric acid, a slight shift of all the protons corresponding to compound **2a** was observed, which confirm that the proposed mechanism involves the electrostatic interaction (N...H—O) between compound **2a** and picric acid (Fig. S11†). Our efforts to get co-crystals of compounds **2a** and (or) **2b** with picric acid were not fruitful. To gain more insights about the interactions involved between **2a** (or) **2b** with PA, we performed DFT calculations. Both, **2a-PA** and **2b-PA** were optimized using 6-31(d,p) basis set, and the optimized molecular structures are presented in Fig. 5. Both the optimized **2a-PA** and **2b-PA** showed weak H-bond interaction between PA and

compounds **2a** & **2b**, thus helps to stabilize the complex formed between the PA and the compounds **2a** & **2b**. The HOMO–LUMO energy difference of **2a** (3.97 eV) and **2b** (3.78 eV) are considerably reduced upon forming a complex with picric acid (2.77 eV for **2a**-PA & 2.55 eV for **2b**-PA). The HOMO of **2a**-PA and **2b**-PA is localized on **2a** or **2b**, whereas the LUMO is localized on picric acid, which suggest that photoinduced electron transfer occurs from **2a** (or) **2b** to picric acid (Table S6†).

Optical nonlinearities

Griesbeck *et al.* showed that three-coordinated boron compounds possess small dipole moment in ground state and large dipole moment in first excited singlet state. In addition, they have tendency to show intense intramolecular charge-transfer transitions when attached with a suitable electron enrich chromophore which can greatly enhance the probability of nonlinear absorption.^{5c} In order to investigate the nonlinear optical behaviour and subsequently, determine the nonlinear absorption coefficient (β) and nonlinear refractive index (n_2), we used the single beam Z-scan technique.¹⁶ The details about the experimental setup could be found elsewhere.¹⁷ In order to measure n_2 and β , we irradiated the solution (concentration: 0.04 mM in dichloromethane) to an intense laser beam from Yb-doped ultrashort pulse ($\Delta\tau = 370$ fs) fiber laser (Model: Cazadero, M/S Calmar Inc., USA) at wavelength of $\lambda = 515$ nm and at 1 kHz repetition rate. The solution was contained in a 1.0 mm thick optical cell which was translated across the focal point of the focused Gaussian laser beam along the beam propagation direction. In closed-aperture (CA) Z-scan, the optical power of transmitted beam from the sample is recorded through a finite-size circular aperture which is placed in the far field. For an open aperture (OA) Z-scan, the entire laser beam transmitted through the sample is measured. Fig. 6 shows the normalized transmittance of CA and OA in the Z-scan experiment for compounds **2a** and **2b**.

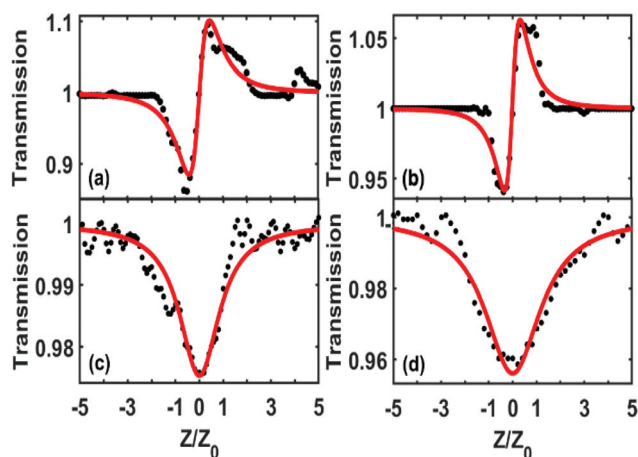


Fig. 6 Normalized Z-scan (a and b) CA transmittance. (c and d) OA transmittance of **2a** and **2b** respectively in CH_2Cl_2 .

The measured normalised z-dependent transmission is represented by black dots. It is to be noted that the laser intensity (I) is relatively small and uniform in the regions which are far from the focal point. This leads to a negligible nonlinear optical absorption ($\text{NLA} = \beta I$) in this region and consequently, the actual transmission is normalised with respect to this value of transmission (far from focal point). Near the focal point, the nonlinear optical effects are more pronounced, which results in significant alternation in transmission.

It is to note that the CA normalized transmission in Fig. 6(a) and (b) exhibits a familiar valley–peak behaviour which indicates a self-focusing behaviour in both the compounds **2a** and **2b**. Alternately, the variation of normalized transmittance results in a positive value of n_2 , thereby depicting a strong electrostrictive effect. According to this, both the compounds exhibit a tendency to have a higher density in regions where the laser intensity is high and consequently, such compounds are expected to offer resistance to thermal lensing effect. In order to estimate the values of n_2 , the experimental measurements have been fitted with the mathematical relation given by,¹⁸

$$T(z, \Delta\phi_0) = 1 - \frac{4\Delta\phi_0 x}{(x^2 + 9)(x^2 + 1)} - \frac{2(x^2 + 3)\Delta\Psi_0}{(x^2 + 9)(x^2 + 1)} \quad (1)$$

where T represents the normalised transmittance, $x = z/z_0$, z_0 being Rayleigh range. $\Delta\phi_0$ is the on-axis phase-shift. The value of n_2 can be estimated by the relation $\Delta\phi_0 = kn_2 I_0 L_{\text{eff}}$, $k = 2\pi/\lambda$ is the wave vector and λ is the pump wavelength, $\Delta\Psi_0 = \beta I_0 L_{\text{eff}}/2$ is the phase change due to nonlinear absorption. It is worthwhile to point out that NLA has been included in eqn (1) so as to account for any kind of asymmetric behaviour. Fig. 6(c and d) shows the normalized transmission for the OA Z-scan measurement. There is an apparent transmission drop at the focus ($z = 0$) for the compounds **2a** and **2b**. Transmission drop near the focus is essentially a consequence of two-photon absorption (TPA) or multi-photon absorption (MPA) which is characterized by a positive value of β . In absence of other nonlinear optical effects or parasitic effects, the normalized transmission is symmetric with respect to the focus ($z = 0$), where it has a minimum transmission.

The absorption coefficient (β) can be estimated from the OA normalized transmission as¹⁶

$$T(z, S = 1) = 1 - \frac{\beta I_0 L_{\text{eff}}}{2^{\frac{1}{2}}(1 + x^2)} \quad (2)$$

where $x = z/z_0$, I_0 is the on-axis peak irradiance at focus ($z = 0$), L_{eff} is the effective sample length. The results are summarized in Table 1 for compounds **2a** and **2b** along with the two-photon absorption cross-section (TPAC) in GM units ($1 \text{ GM} = 10^{-50} \text{ cm}^4 \text{ s per photon}$).

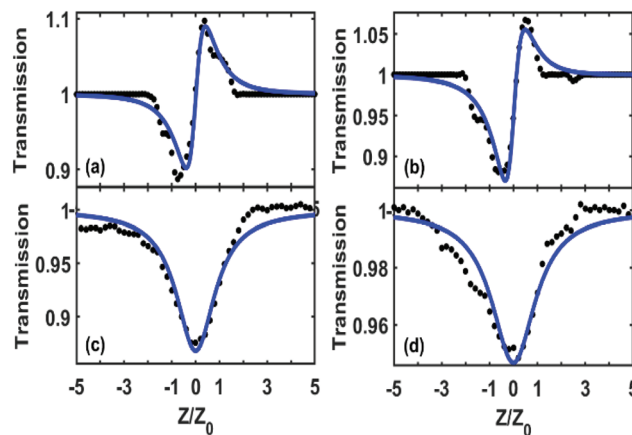
Recently, there have been a concerted effort to identify and ascertain a plausible mechanism behind the high nonlinearity in PA coordinated crystals. However, such investigations have rarely been carried out in the context of PA in solutions where the flexibility in realizing π -conjugations are significantly

Table 1 Optical nonlinear coefficients of **2a** and **2b** at 1 kHz repetition rates

Compound	n_2 ($\times 10^{-16}$ cm ² W ⁻¹)	β ($\times 10^{-12}$ cm W ⁻¹)	TPAC (GM)
2a (w/o picric acid)	2.3	2.0	7
2b (w/o picric acid)	1.14	4.0	13
Picric acid	—	6.59	23
2a (with 7% picric acid)	1.73	10.9	38
2b (with 14% picric acid)	1.9	4.8	17
2b (with 40% picric acid)	—	25.1	66

higher. It has been pointed out by Karthikeyan *et al.* that NO₂ and OH groups in PA are discernibly easy to polarise. Consequently, PA interact with nearby species through rapid charge delocalization.¹⁹ It is worthwhile to note that the presence of three electron withdrawing NO₂ groups in PA makes it a good π -acceptor for neutral carrier donor molecule. However, NO₂ group present at the *para*-position exhibits maximum charge delocalization which gives rise to the possibility of a longer conjugation length when interacts with electron-donating species. Thus, detection of PA through enhancing the non-linear optical interactions could be plausible option. In order to investigate this aspect, we measured the nonlinear optical coefficients for pure PA solution which resulted in $\beta = 6.59 \times 10^{-12}$ cm W⁻¹. This value is higher than the compounds **2a** and **2b** which could be attributed to the presence of phenolic (OH) group. This favours the formation of hydrogen-bonding interactions, which leads to increased molecular hyperpolarizability.²⁰ In our work, we observed the fluorescence quenching on addition of PA to the pyrazole anchored boron fluorophore which encouraged us to have a further investigation of how does it affect the nonlinearity of these compounds. Since, PA is explosive in nature, we have added limited concentrations (7.0 equiv. and 14.0 equiv. to the compounds **2a** and **2b** respectively). This concentration quenches the fluorescence of each solution by approximately 40%. The normalized CA and OA transmittance of compounds **2a** and **2b** after adding PA is shown below.

It is evident from the Fig. 7(a) and (b) above, that the addition of PA does not change the behaviour of the CA transmittance and hence, it does change the sign of n_2 for **2a** as well as **2b**. From Table 1, it could be observed that there is a marginal change in the value of n_2 with the addition of 7.0 equiv. of PA in **2a** and **2b** which indicates that the optical phase changes are insignificant. On the other hand, we observed a significant change in the value of β in case of **2a**. For 7.0 equiv. PA addition to **2a**, we observed more than five-fold increase in the value of β . This change can be attributed to the significant alteration in π -conjugation of the compound due to the association of OH from PA to the lone pair of electrons at nitrogen in pyrazole. In case of **2b**, however, there is small change in the value of β after addition of 14.0 equiv. of PA. Further, β increases significantly with increase in PA concentration. In fact, we observed that $\beta = 25.1 \times 10^{-12}$ cm W⁻¹ when 40.0 equiv. PA is added to **2b**. At low PA concentration,

**Fig. 7** Normalized Z-scan (a and b) CA transmittance. (c and d) OA transmittance after adding 7.0 equiv. and 14.0 equiv. PA in compounds **2a** and **2b** respectively. Solvent: CH₂Cl₂.

the probability of the formation of **2b**-PA is appreciably small, however, at high PA concentration the equilibrium shifts to form **2b**-PA *via* intermolecular hydrogen bond, which, in turn results in a gradual increase in the effective conjugation length. For a comparison, we have listed the values of n_2 and β for some similar organic compounds in Table S8.† The comparison reveals that **2a** and **2b** possesses appreciable third-order nonlinear response which scales up higher with the addition of picric acid. Table S8† also presents a few measurements which were carried out using continuous-wave (CW) laser which yields exceptionally high values of NLO coefficients due to large thermo-optic manifestations. Therefore, NLO measurements and material stability of compounds **2a** and **2b** suggest that they are potential candidates for optical switching and limiting applications. To probe the effect of triarylborane linkage with triaryl pyrazole, we synthesized triaryl pyrazole¹⁵ and studied its photophysical properties. Although, the quenching phenomenon was similar to that of **2a**, the observed absolute quantum yield was lower than that of **2a**, which is the advantage of linking triaryl pyrazole with triarylborane.

Experimental section

Synthesis of compound 1a

To a solution of 4-bromo phenylhydrazine (5.48 g, 29.30 mmol) and 1,3-diphenylpropane-1,3-dione (5.00 g, 22.30 mmol) in methanol (80 mL) was added AcOH (80 mL). The reaction mixture was heated to reflux for 24 h. After cooling to RT, the mixture was poured into water and extracted with CH₂Cl₂. The combined extracts were washed with saturated sodium carbonate solution followed by brine and dried over anhydrous Na₂SO₄. Solvent was removed under reduced pressure and the residue was purified by silica gel column chromatography using ethyl acetate and *n*-hexane as eluent. Yield: 6.28 g, (75%). Mp: 280 °C. ¹H NMR (400 MHz, CDCl₃): δ

= 7.99 (d, J = 7.5 Hz, 2H), 7.51–7.47 (m, 4H), 7.43–7.28 (m, 8H), 6.86 (s, 1H). ^{13}C NMR (100 MHz, CDCl_3): δ = 152.27, 144.36, 139.14, 132.83, 131.98, 130.30, 128.76, 128.72, 128.66, 128.55, 128.18, 126.54, 125.83, 120.92, 105.70. HR-MS (ESI): calcd for $\text{C}_{21}\text{H}_{15}\text{Br}_1\text{N}_2$ ($[\text{M} + \text{H}]^+$): 375.0491, found: 375.0464.

Synthesis of compound 2a

Compound **1a** (4.41 g, 11.75 mmol) was dissolved in anhydrous THF (150 mL) under nitrogen atmosphere and the resulting solution was cooled to -78°C with stirring. Then, *n*-butyllithium (8.1 mL, 12.93 mmol, 1.6 M solution in hexane) was slowly added to the stirred solution over 20 min. After 1 h, a solution of dimesitylfluoroborane (3.47 g, 12.93 mmol) in 35 mL of dry THF was added over 10 min. The reaction mixture was allowed to warm to room temperature and stirred for 24 h. After 24 h, water was added to the reaction mixture and extracted with ethyl acetate. The combined extracts were washed with brine and dried over anhydrous Na_2SO_4 . Solvent was removed under reduced pressure and the obtained residue was purified by silica gel column chromatography using ethyl acetate and *n*-hexane as eluent. Yield: 4.67 g, (73%). Mp: 192°C . ^1H NMR (400 MHz, CDCl_3): δ = 8.02 (d, J = 7.5 Hz, 2H), 7.59 (d, J = 8.1 Hz, 2H), 7.50 (t, J = 7.5 Hz, 2H), 7.45–7.35 (m, 8H), 6.91 (s, 5H), 2.38 (s, 6H), 2.11 (s, 12H). ^{13}C NMR (100 MHz, CDCl_3): δ = 152.43, 144.86, 144.70, 142.79, 141.61, 140.87, 138.91, 137.13, 133.00, 130.66, 128.89, 128.75, 128.53, 128.49, 128.36, 128.21, 125.96, 124.64, 105.75, 23.55, 21.31. HR-MS (ESI): calcd for $\text{C}_{39}\text{H}_{37}\text{B}_1\text{N}_2$ ($[\text{M} + \text{H}]^+$): 545.3129, found: 545.3138.

Synthesis of compound Th-Pz-diPh

To a mixture of 3,5-diphenyl-1H-pyrazole, (6.00 g, 27.24 mmol), 2-bromo thiophene (3.91 mL, 40.86 mmol), Cu_2O (389 mg, 2.724 mmol), Cs_2CO_3 (9.76 g, 29.96 mmol) was added degassed dry DMF under nitrogen atmosphere. The reaction mixture was heated at reflux for 48 h. After cooling to room temperature, 200 mL of H_2O and 200 mL of CH_2Cl_2 were added, and the phases were separated. The aqueous phase was extracted with (3×75 mL) of CH_2Cl_2 and the combined organic phases were dried over Na_2SO_4 , and the solvent was removed under reduced pressure. The obtained residue was purified by silica gel column chromatography using ethyl acetate and *n*-hexane as eluent. Yield: 3.95 g, (48%). Mp: 132°C . ^1H NMR (400 MHz, CDCl_3): δ = 7.93 (d, J = 8 Hz, 2H), 7.47–7.35 (m, 8H), 7.14 (d, J = 8 Hz, 1H), 6.87–6.84 (m, 1H), 6.81 (s, 1H), 6.75 (d, J = 4 Hz, 1H). ^{13}C NMR (100 MHz, CDCl_3): δ = 152.45, 145.75, 142.22, 132.70, 130.10, 128.98, 128.88, 128.78, 128.60, 128.37, 126.04, 125.65, 123.05, 121.75, 105.39. HR-MS (ESI): calcd for $\text{C}_{19}\text{H}_{14}\text{N}_2\text{S}$ ($[\text{M} + \text{H}]^+$): 303.0950, found: 303.0945.

Synthesis of compound 1b

Compound **Th-Pz-diPh** (3.50 g, 11.57 mmol) was dissolved in 80 mL and *N*-bromosuccinimide (2.26 g, 12.70 mmol) was added. Then the reaction mixture was stirred for 24 h in dark condition. To this mixture, 100 mL of H_2O and 70 mL of

CH_2Cl_2 were added to the mixture and the organic phase was collected and the aqueous phase extracted with (2×50 mL) of CH_2Cl_2 . The combined organic phases were dried over Na_2SO_4 , and solvent was removed under reduced pressure. The obtained residue was purified by silica gel column chromatography using ethyl acetate and *n*-hexane as eluent. Yield: 3.96 g, (90%). Mp: 138°C . ^1H NMR (400 MHz, CDCl_3): δ = 7.92 (d, J = 7.1 Hz, 2H), 7.48–7.36 (m, 8H), 6.82 (d, J = 4.0 Hz, 1H), 6.78 (s, 1H), 6.44 (d, J = 4.0 Hz, 1H). ^{13}C NMR (100 MHz, CDCl_3): δ = 152.77, 145.54, 142.64, 132.44, 129.77, 129.19, 129.07, 128.85, 128.79, 128.57, 128.43, 126.05, 121.29, 109.77, 105.77. HR-MS (ESI): calcd for $\text{C}_{19}\text{H}_{13}\text{N}_2\text{SBr}$ ($[\text{M} + \text{H}]^+$): 381.0056, found: 381.0052.

Synthesis of compound 2b

Compound **2b** was prepared by following a procedure similar to that used for compound **2a**. The quantities involved are as follows: Compound **1b** (3.00 g, 7.87 mmol), *n*-butyllithium (5.41 mL, 8.66 mmol, 1.6 M solution in hexane), dimesitylfluoroborane (2.32 g, 8.66 mmol). Yield: 2.38 g, (55%). Mp: 192°C . ^1H NMR (400 MHz, CDCl_3): δ = 7.91 (d, J = 7.2, 8.0 Hz, 2H), 7.46–7.34 (m, 8H), 7.18 (d, J = 4 Hz, 1H), 6.82 (s, 4H), 6.78 (s, 1H), 6.75 (d, J = 3.9 Hz, 1H), 2.31 (s, 6H), 2.14 (s, 12H). ^{13}C NMR (100 MHz, CDCl_3): δ = 153.87, 152.87, 145.33, 140.94, 139.71, 138.71, 132.45, 130.16, 129.31, 129.19, 128.80, 128.70, 128.54, 128.30, 126.12, 121.80, 106.53, 23.58, 21.33. HR-MS (ESI): calcd for $\text{C}_{37}\text{H}_{35}\text{N}_2\text{SB}$ ($[\text{M} + \text{H}]^+$): 551.2693, found: 551.2701.

Conclusions

In summary, 3,5-diphenylpyrazole anchored tri-coordinated boron compounds have been synthesized. The fluorescence studies revealed that compounds **2a** and **2b** are highly selective and sensitive for the detection of picric acid. The presence of 3,5-diphenyl pyrazole moiety endowed our design to have the potential to discriminate picric acid over other analytes. Subsequently, we measured the NLO properties (namely n_2 and β) for the compounds **2a** and **2b** which revealed a direct dependence on addition of concentration of PA to the solution. The addition of PA essentially provides a plausible route to enhance the effective conjugation length of the compounds thereby, larger values of nonlinear optical coefficients. In future, it would be worthwhile to investigate and corroborate the precise impact of quenching of linear absorption due to PA addition on the nonlinear absorption. The results presented here hold a great capability for development of new selective chemosensors based on tri-coordinated boron system.

Conflicts of interest

There are no conflicts to declare.

Acknowledgements

The authors thank Science & Engineering Research Board (SERB) (EMR/2017/000620), New Delhi and Department of Atomic Energy (DAE) for financial support.

Notes and references

- (a) F. Jäkle, *Chem. Rev.*, 2010, **110**, 3985–4022; (b) M. Elbing and G. C. Bazan, *Angew. Chem., Int. Ed.*, 2008, **47**, 834–838; (c) F. P. Gabbai, *Angew. Chem., Int. Ed.*, 2012, **51**, 6316–6318; (d) S. Y. Li, Z. B. Sun and C. H. Zhao, *Inorg. Chem.*, 2017, **56**, 8705–8717; (e) S. K. Mellerup and S. Wang, *Trends Chem.*, 2019, **1**, 77–89; (f) E. Grotthuss, A. John, T. Kaese and M. Wagner, *Asian J. Org. Chem.*, 2018, **7**, 37–53; (g) S. Kirschner, J.-M. Mewes, M. Bolte, H.-W. Lerner, A. Dreuw and M. Wagner, *Chem. – Eur. J.*, 2017, **23**, 5104–5116; (h) A. John, M. Bolte, H. W. Lerner and M. Wagner, *Angew. Chem., Int. Ed.*, 2017, **56**, 5588–5592; (i) L. G. Mercier, W. E. Piers and M. Parvez, *Angew. Chem., Int. Ed.*, 2009, **48**, 6108–6111; (j) K. Hu, Z. Zhang, J. Burke and Y. Qin, *J. Am. Chem. Soc.*, 2017, **139**, 11004–11007; (k) R. Yoshii, A. Hirose, K. Tanaka and Y. Chujo, *J. Am. Chem. Soc.*, 2014, **136**, 18131–18139; (l) T. Kushida, A. Shuto, M. Yoshio, T. Kato and S. Yamaguchi, *Angew. Chem., Int. Ed.*, 2015, **54**, 6922–6925; (m) A. Escande and M. J. Ingleson, *Chem. Commun.*, 2015, **51**, 6257–6274; (n) X. Y. Wang, J. Y. Wang and J. Pei, *Chem. – Eur. J.*, 2015, **21**, 3528–3539.
- (a) S. K. Mellerup and S. Wang, *Chem. Soc. Rev.*, 2019, **48**, 3537–3549; (b) U. P. Pandey and P. Thilagar, *Adv. Opt. Mater.*, 2020, 1902145; (c) N. A. Riensch, L. Fritze, T. Schindler, M. Kremer and H. Helten, *Dalton Trans.*, 2018, **47**, 10399–10403; (d) H. Lin, S. Patel and F. Jäkle, *Macromolecules*, 2020, **53**, 10601–10612.
- (a) L. Ji, S. Griesbeck and T. B. Marder, *Chem. Sci.*, 2017, **8**, 846–863; (b) S. Pagidi, N. K. Kalluvettukuzhy and P. Thilagar, *Inorg. Chem.*, 2020, **59**, 3142–3151; (c) K. Yuan, R. J. Kahan, C. Si, A. Williams, S. Kirschner, M. Uzelac, E. Zysman-Colman and M. Ingleson, *Chem. Sci.*, 2020, **11**, 3258–3267; (d) K. Mishiba, Y. Tanaka and M. Akita, *Chem. – Eur. J.*, 2021, **27**, 1–8.
- L. Ji, I. Krummenacher, A. Friedrich, A. Lorbach, M. Haehnel, K. Edkins, H. Braunschweig and T. B. Marder, *J. Org. Chem.*, 2018, **83**, 3599–3606.
- (a) Z. Yuan, C. D. Entwistle, J. C. Collings, D. Albesa-Jové, A. S. Batsanov, J. A. K. Howard, N. J. Taylor, H. M. Kaiser, D. E. Kaufmann, S.-Y. Poon, W.-Y. Wong, C. Jardin, S. Fathallah, A. Boucekkine, J.-F. Halet and T. B. Marder, *Chem. – Eur. J.*, 2006, **12**, 2758–2771; (b) J. C. Collings, S.-Y. Poon, C. L. Droumaguet, M. Charlot, C. Katan, L.-O. Palsson, A. Beeby, J. A. Mosely, H. M. Kaiser, D. Kaufmann, W.-Y. Wong, M. Blanchard-Desce and T. B. Marder, *Chem. – Eur. J.*, 2009, **15**, 198–208; (c) S. Griesbeck, E. Michail, F. Rauch, H. Ogasawara, C. Wang, Y. Sato, R. M. Edkins, Z. Zhang, M. Taki, C. Lambert, S. Yamaguchi and T. B. Marder, *Chem. – Eur. J.*, 2019, **25**, 13164–13175; (d) S. Griesbeck, E. Michail, C. Wang, H. Ogasawara, S. Lorenzen, L. Gerstner, T. Zang, J. Nitsch, Y. Sato, M. Taki, C. Lambert, S. Yamaguchi and T. B. Marder, *Chem. Sci.*, 2019, **10**, 5405–5422.
- (a) R. Stahl, C. Lambert, C. Kaiser, R. Wortmann and R. Jakober, *Chem. – Eur. J.*, 2006, **12**, 2358–2370; (b) D. Reitzenstein and C. Lambert, *Macromolecules*, 2009, **42**, 773–782.
- Z.-Q. Liu, Q. Fang, D.-X. Cao, D. Wang and G.-B. Xu, *Org. Lett.*, 2004, **6**, 2933–2936.
- A. Proń, M. Baumgarten and K. Mullen, *Org. Lett.*, 2010, **12**, 4236–4239.
- P. Chen, A. S. Marshall, S.-H. Chi, X. Yin, J. W. Perry and F. Jäkle, *Chem. – Eur. J.*, 2015, **21**, 18237–18247.
- F. Zhang, T. Noda, H. Kageyama and Y. Shirota, *Proc. SPIE*, 2009, **7213**(1–5), 721302.
- (a) S. Yamaguchi, S. Akiyama and K. Tamao, *J. Am. Chem. Soc.*, 2001, **123**, 11372–11375; (b) K. Parab, K. Venkatasubbaiah and F. Jäkle, *J. Am. Chem. Soc.*, 2006, **128**, 12879–12885; (c) S. K. Mellerup, Y.-L. Rao, H. Amarne and S. Wang, *Org. Lett.*, 2016, **18**, 4436–4439; (d) A. L. Brazeau, K. Yuan, S.-B. Ko, I. Wyman and S. Wang, *ACS Omega*, 2017, **2**, 8625–8632; (e) C. A. Swamy, P. S. Mukherjee and P. Thilagar, *Inorg. Chem.*, 2014, **53**, 4813–4823; (f) H. Lee, S. Jana, J. Kim, S. U. Lee and M. H. Lee, *Inorg. Chem.*, 2020, **59**, 1414–1423.
- (a) J. S. Caygill, F. Davi and S. P. J. Higson, *Talanta*, 2012, **88**, 14–29; (b) Y. Salinas, R. Martinez-Manez, M. D. Marcos, F. Sancenon, A. M. Costero, M. Parra and S. Gil, *Chem. Soc. Rev.*, 2012, **41**, 1261–1296; (c) M. E. Germain and M. J. Knapp, *Chem. Soc. Rev.*, 2009, **38**, 2543–2555; (d) H. Sohn, R. M. Calhoun, M. J. Sailor and W. C. Trogler, *Angew. Chem., Int. Ed.*, 2001, **40**, 2104–2105; (e) J. Akhavan, *The Chemistry of Explosives*, The Royal Society of Chemistry, London, 2nd edn, 2004.
- (a) P. C. Ashbrook and T. A. Houts, *Chem. Health Saf.*, 2003, **10**, 27; (b) K. M. Wollin and H. H. Dieter, *Arch. Environ. Contam. Toxicol.*, 2005, **49**, 18–26.
- (a) M. Hengchang, Z. Zhongwei, J. Yuanyuan, Z. Lajia, Q. Chunxuan, C. Haiying, Y. Zengming, Y. Zhiwang and L. Ziqiang, *RSC Adv.*, 2015, **5**, 87157–87167; (b) S. Areti, S. Bandaru, R. Kandi and C. P. Rao, *ACS Omega*, 2019, **4**, 1167–1177; (c) Q. Lin, X.-W. Guan, Y.-Q. Fan, J. Wang, L. Liu, J. Liu, H. Yao, Y.-M. Zhang and T.-B. Wei, *New J. Chem.*, 2019, **43**, 2030–2036; (d) S. Madhu, A. Bandela and M. Ravikanth, *RSC Adv.*, 2014, **4**, 7120–7123; (e) H. Sohn, M. J. Sailor, D. Magde and W. C. Trogler, *J. Am. Chem. Soc.*, 2003, **125**, 3821–3830; (f) J. Liu, Y. Zhong, P. Lu, Y. Hong, J. W. Y. Lam, M. Faisal, Y. Yu, K. S. Wong and B. Z. Tang, *Polym. Chem.*, 2010, **1**, 426–429; (g) S. Shanmugaraju and P. S. Mukherjee, *Chem. Commun.*, 2015, **51**, 16014–16032; (h) A. S. Tanwar, S. Hussain, A. H. Malik, M. A. Afroz and P. K. Iyer, *ACS Sens.*, 2016, **1**, 1070–1077; (i) K. Dhanunjayarao, V. Mukundam and

- K. Venkatasubbaiah, *Inorg. Chem.*, 2016, **55**, 11153–11159; (j) V. Mukundam, A. Kumar, K. Dhanunjayarao, A. Ravi, S. Peruncheralathan and K. Venkatasubbaiah, *Polym. Chem.*, 2015, **6**, 7764–7770; (k) V. Mukundam, K. Dhanunjayarao, R. Mamidala and K. Venkatasubbaiah, *J. Mater. Chem. C*, 2016, **4**, 3523–3530.
- 15 V. Mukundam, S. Sa, A. Kumari, R. Das and K. Venkatasubbaiah, *J. Mater. Chem. C*, 2019, **7**, 12725–12737.
- 16 M. S. Bahae, A. A. Said, T. H. Wei, D. J. Hagan and E. W. V. Stryland, *IEEE J. Quantum Electron.*, 1990, **26**, 760–769.
- 17 M. Vanga, S. Sa, A. Kumari, A. C. Murali, P. Nayak, R. Das and K. Venkatasubbaiah, *Dalton Trans.*, 2020, **49**, 7737–7746.
- 18 M. Yin, H. Li, S. H. Tang and W. Ji, *Appl. Phys. B*, 2000, **70**, 587.
- 19 K. V. Karthikeyan, S. Anandhi, V. Ramkumar, T. S. Shyju, S. N. Jaisankar and R. Suriakarthick, *Mater. Res. Express*, 2019, **6**, 075105.
- 20 M. Manonmani, C. Balakrishnan, S. R. Ahamed, G. Vinitha, S. P. Meenakshisundaram and R. M. Sockalingam, *J. Mol. Struct.*, 2019, **1190**, 1–10.